Revisiting Pb isotope signatures of Ni-Fe alloy hosted by antigorite serpentinite from the Josephine Ophiolite, USA

Mayu KAKEFUDA[*], Tatsuki TSUJIMORI[*,**,***], Katsuyuki YAMASHITA[†], Yoshiyuki IIZUKA[**,‡] and Kennet E. FLORES[**,***,§]

[*]*Department of Earth Science, Tohoku University, Sendai 980-8578, Japan*
[**]*Center for Northeast Asian Studies, Tohoku University, Sendai 980-8576, Japan*
[***]*Department of Earth and Planetary Sciences, American Museum of Natural History, New York, NY 10024-5192, USA*
[†]*Graduate School of Natural Science and Technology, Okayama University, Okayama 700-8530, Japan*
[‡]*Institute of Earth Sciences, Academia Sinica, Taipei 11529, Taiwan*
[§]*Department of Earth and Environmental Sciences, Brooklyn College of the City University of New York, Brooklyn, NY 11210, USA*

Awaruite ($Ni_{2-3}Fe$) is a natural occurring Ni-Fe alloy in serpentinite, which represents a better candidate to assess Pb isotope signatures in the mantle wedge since the concentration of Pb in awaruite is almost ten times higher than that in serpentine minerals. Revisiting so-called josephinite from the Josephine Ophiolite confirmed that josephinite is characterized by aggregates of awaruite with minor Ni-arsenide. The Raman spectrum obtained from the josephinite-hosting serpentinite shows diagnostic peaks of antigorite, suggesting josephinite might have formed under stability field of antigorite. Using a stepwise leaching and partial dissolution method, we obtained Pb isotope ratios of josephinite by TIMS. Since all ratios converged to a homogeneous value towards the later steps of the partial dissolution, this allowed to calculate weighted mean values that give precise Pb isotope ratios: $^{206}Pb/^{204}Pb$ = 18.3283 ± 0.0020 (MSWD = 0.49), $^{207}Pb/^{204}Pb$ = 15.5645 ± 0.0020 (MSWD = 0.36), and $^{208}Pb/^{204}Pb$ = 38.0723 ± 0.0061 (MSWD = 0.50); these values can be evaluated as one of the reference Pb isotope ratios in serpentinites from supra-subduction zone ophiolite. The newly obtained Pb isotope ratios of josephinite are consistent with the previous reported isotope ratios, which are characterized by enriched $^{207}Pb/^{204}Pb$ ratio with MORB-source like $^{206}Pb/^{204}Pb$ and $^{208}Pb/^{204}Pb$ ratios. Although these Pb isotope features interpreted as a reflection of arc magmatism in the previous study, the presence of Ni-arsenide and enriched $^{207}Pb/^{204}Pb$ ratios may indicate an involvement of As-rich fluids derived from slab sediments.

Keywords: Josephinite, Awaruite, Pb isotope ratios, Serpentinite, Josephine Ophiolite

INTRODUCTION

During last two decades, serpentinite and serpentinization of mantle peridotite have received much attention for their important roles in mineralogical, geochemical, and seismological processes (e.g., Evans et al., 2013; Oyanagi et al., 2015; Plümper et al., 2017; Yamada et al., 2019a). One of those notable roles played by serpentinites is their contribution on discussing the fluid-mediated material transfer at convergent plate boundaries. In tectonic context, serpentinite can be a major storage of fluid-mobile elements such as B, W, As, and Sb, as well as alkaline elements, released from subducting slabs (e.g., Hattori et al., 2005; Martin et al., 2011; Kodolányi et al., 2012; Deschamps and Hattori, 2013; Guillot and Hattori, 2013; Peters et al., 2017). Consequently, the dehydration of subducted serpentinites takes on a significant role for deriving both large amounts of water and fluid-mobile elements to the deep mantle (e.g., Scambelluri et al., 2004; Reynard, 2013; Guillot et al., 2015; Debret and Sverjensky, 2017). Infiltration of hydrothermal fluids into serpentinite and serpentinized peridotite also cause ore mineralization enriched in S, Ni, Fe, and Co (e.g., Kamenetsky et al., 2016). Such mineralization is highly controlled by elemental saturation as well as oxygen fugacity (f_{O_2}), sulfur fugacity (f_{S_2} or Eh) and silica activity.

doi:10.2465/jmps.190731a
M. Kakefuda, mayu.kakefuda.r4@dc.tohoku.ac.jp Corresponding author:
T. Tsujimori, tatsukix@tohoku.ac.jp

Advance Publication Article

Understanding fluid-mediated processes in serpentinites acquires considerable importance in various fields of geoscience. For example, characterization of the fluid evolution and material transfer from slab dehydration to the mantle wedge is a key step to understand the large-scale elemental cycles within the solid Earth. The supra-subduction zone (SSZ) processes, including mantle wedge serpentinization, are essentially triggered by prograde dehydration of the subducting slabs. Geochemical studies of SSZ serpentinites thus seem to be necessary for understanding the dynamics of fluids at active margins. As part of our current geochemical reconnaissance study of serpentinites in various geologic settings (e.g., Yamada et al., 2019a, 2019b), this contribution focuses on exceptional aggregates of serpentinite-hosted Ni-Fe alloy, so-called josephinite, from the Josephine Ophiolite, Oregon, USA (e.g., Botto and Morrison, 1976; Göpel et al., 1990; Britten et al., 2017). The Josephine Ophiolite has been known as a volcanic arc-type SSZ ophiolite in the circum-Pacific (Fig. 1) (cf. Dilek and Furnes, 2011).

Göpel et al. (1990) was the first to report Pb isotope ratios of josephinite. They reported the similarity of Pb isotope ratios of josephinite and those of the diorite intrusions in the Josephine Ophiolite and suggested the involvement of hydrothermal fluids associated with the intrusions to the formation of josephinite. In order to re-characterize fluids that evolved and formed josephinite in serpentinites, in this study, we have carried out both mineralogical investigation and Pb isotope analysis using weighted mean method to josephinite. Using our new data and pre-existing data by Göpel et al. (1990), we present the possibility of a sediment-derived fluid involvement in the josephinite formation.

PREVIOUS STUDIES AND LEAD ISOTOPE COMPOSITION OF JOSEPHINITE

Josephinite is a nearly monomineralic, metallic rock composed mainly of Ni-Fe alloy called awaruite, with minor amount of Ni-arsenides (e.g., Botto and Morrison, 1976). The rock has been found mainly as nuggets in alluvial placers and as rare in-situ clots in serpentinites of the Josephine Ophiolite. The Josephine Ophiolite is a Jurassic oceanic crust sequence of an intra-oceanic arc or back-arc setting tectonic origin (Fig. 1). The ophiolite consists of harzburgitic residual peridotite (the Josephine Peridotite), serpentinized peridotite, ultramafic-mafic cumulates, gabbro, sheeted dike complex, pillow basalt, and coeval diorite intrusions (Dick, 1974; Harper, 1984; Kelemen and Dick, 1995; Le Roux et al., 2014). Because of the unusually large size of naturally occurring Ni-Fe alloy found in the near surface environment, the origin of josephinite have raised scientific controversy, whether it came from the Earth's core, since the late 1970s (e.g., Dick, 1974; Bird and Weathers, 1979).

Göpel et al. (1990) determined Pb isotope ratios of three josephinite samples using a partial dissolution method. The decontaminated metallic samples yielded isotope values of $^{206}Pb/^{204}Pb$ = 18.389-18.547, $^{207}Pb/^{204}Pb$ = 15.570-15.592, and $^{208}Pb/^{204}Pb$ = 38.058-38.102. These values were very close to those of the associated diorite intrusions ($^{206}Pb/^{204}Pb$ = 18.188-18.546, $^{207}Pb/^{204}Pb$ =

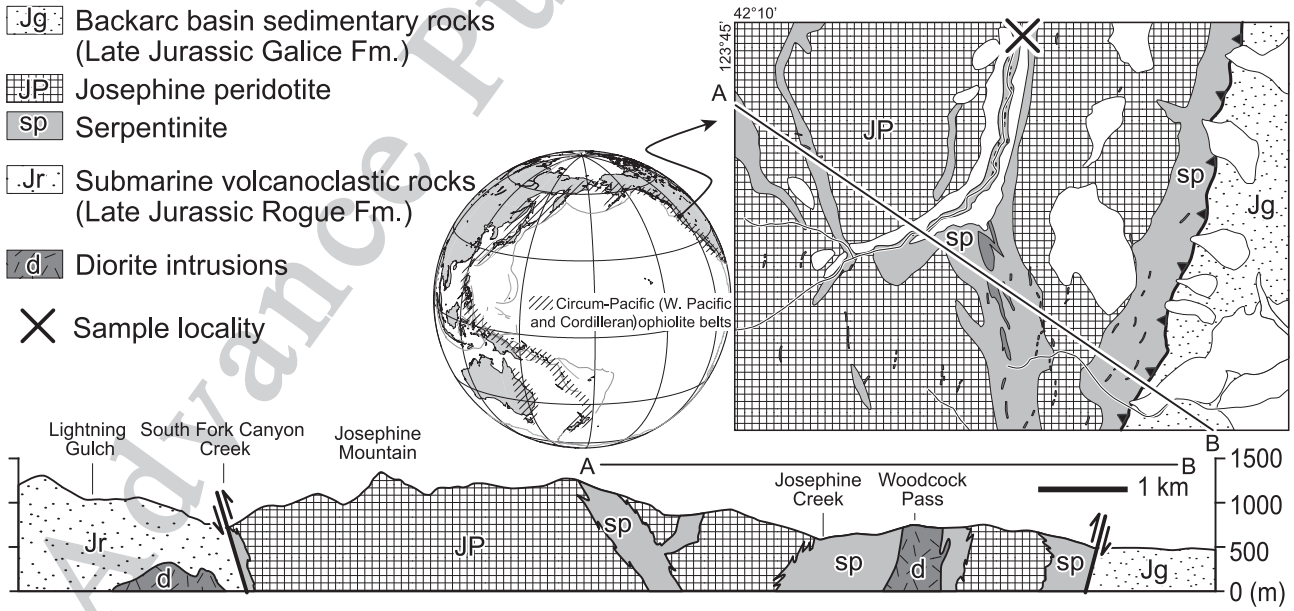

Figure 1. Geologic map and cross-section showing a locality of josephinite-bearing serpentinite of the Josephine Ophiolite, Oregon, USA. The map was modified after Ramp (1986). The cross-section was partially modified after an un-published map drawn by R.G. Coleman.

Advance Publication Article

15.533–15.554, and $^{208}Pb/^{204}Pb$ = 37.852–38.061), however slightly differed from the parent harzburgite ($^{206}Pb/^{204}Pb$ = 17.444–18.257, $^{207}Pb/^{204}Pb$ = 15.543–15.602, and $^{208}Pb/^{204}Pb$ = 37.342–38.048), which was interpreted as a signature of hydrothermal fluids associated with the diorite intrusions. Note that the leachate solutions of josephinite acquired from leaching procedure yielded significantly higher $^{207}Pb/^{204}Pb$ ratios (15.618–15.643) than those from partial dissolution steps.

ANALYTICAL METHODS

Mineralogical characterizations

Preparatory to Pb isotope analysis, an epoxy-mounted and polished josephinite nugget sample JOS was examined mineralogically by a field emission-scanning electron microscope (FE-SEM: JEOL JSM-7100F) equipped with an energy-dispersive spectrometer (EDS: Oxford Instruments Ltd., X-max 80 operated by INCA-350) at Academia Sinica. Major and minor element compositions of awaruite and Ni-arsenide were analyzed by a field emission-electron probe micro analyzer (FE-EPMA: JEOL JXA-8500F) also at Academia Sinica. A 2 μm defocused beam was operated for quantitative analysis at an acceleration voltage of 12 kV and 25 kV with a beam current of 6 nA and 15 nA for silicates and metallic alloys, respectively. Quantitative data were corrected by the methods of Oxide-PRZ and Metal-PRZ for silicates and metallic alloys, respectively. To confirm its oxidation state, and presence of silicate and oxide inclusions in alloy phases, O and silicate related elements such as Si and Al were also analyzed during metal analysis.

In addition, to identify the polymorph of host serpentinite, josephinite-bearing serpentinite sample SRP was investigated by a confocal Raman microscope (HORIBA XploRA PLUS) at Tohoku University. A 532 nm solid-state Nd-YAG laser with 10 mW power was used as laser source. The Raman spectra were measured ranging from 199.6 to 1194 cm^{-1} in 1.1 cm^{-1} steps (2400 gr/mm). The diameter of laser spot was ~ 2 μm; the exposure time was 50 s (5 s × 10). The Raman shift was calibrated using a silicon reference.

Pb isotope analysis

The chemical separation of Pb from sample JOS was carried out in a clean laboratory at Okayama University. Sample JOS was first leached in 0.5 N HBr for 5 min at room temperature to remove any superficial contamination. The leaching procedure was repeated six times (L1 to L6). The sample was subsequently dissolved in 1.0 N HBr at 100 °C in 11 steps (PD7 to PD17). The duration of the partial dissolution ranged from 1 h in the first 3 steps (PD7 to PD9), to >10 hours in the last 7 steps (PD11 to PD17). Pb was extracted and purified using HBr-HNO_3 media chemistry modified from Lugmair and Galer (1992). The Pb isotope analyses were performed at Okayama University using a Finnigan MAT 262 thermal-ionization mass spectrometer in a static mode. The Pb isotope ratios were corrected for mass discrimination based on the repeated analyses of NIST 981 standard (See Amelin, 2008 for the NIST 981 values). The reproducibilities for $^{206}Pb/^{204}Pb$, $^{207}Pb/^{204}Pb$, and $^{208}Pb/^{204}Pb$ were 0.039, 0.056, and 0.076% (2σ) respectively. The total analytical blank was sufficiently small (6–18 pg) in comparison to the amount of Pb extracted from sample JOS (70–150 ng for L and 90–500 ng for PD), thus no blank correction was applied.

RESULTS

Textural and mineralogic features

The investigated josephinite sample JOS consists mainly of Ni-Fe alloy; awaruite ($Ni_{2-3}Fe$) (Fig. 2a). The back-scattered electron (BSE) contrast (Fig. 2b) and the crystal orientation analysis by electron back-scatter diffraction indicate that awaruite in josephinite is aggregates of randomly oriented anhedral crystals (~ 0.05–0.1 mm in size). An aggregate of awaruite encloses Ni-arsenide (~ 0.02–0.1 mm in size) (Fig. 2c). Fe and Ni contents of awaruite vary significantly; 23.3–27.6 wt% Fe and 70.5–76.5 wt% Ni; the Ni/(Ni + Fe) atomic ratio ranges from 0.71 to 0.76. Awaruite has a trace amount of Cu (up to 1.2 wt%), Mn (up to 0.02 wt%), As (up to 0.22 wt%), Co (up to 0.67 wt%), and S (up to 0.40 wt%). Ni-arsenide enclosed in awaruite has a composition of 67.0–68.3 wt% Ni and 31.6–32.2 wt% As with trace amount of Fe (up to 2.2 wt%), Mn (up to 0.02 wt%), and Co (up to 0.01 wt%). Representative chemical compositions of awaruite and Ni-arsenide in sample JOS are shown in Tables 1 and 2, respectively.

The Raman spectrum obtained from sample SRP shows diagnostic peaks at ~ 227, ~ 373, ~ 683, ~ 1036, ~ 3664, and ~ 3694 cm^{-1} (Fig. 3), indicating that host serpentinites composed mainly of antigorite. Note that no lizardite was found from any investigated host serpentinites. See Table 3 for the representative chemical composition of antigorite in SRP.

Pb isotope ratios

The obtained Pb isotope ratios ($^{206}Pb/^{204}Pb$, $^{207}Pb/^{204}Pb$, and $^{208}Pb/^{204}Pb$) from sample JOS are listed in Table 4

Advance Publication Article

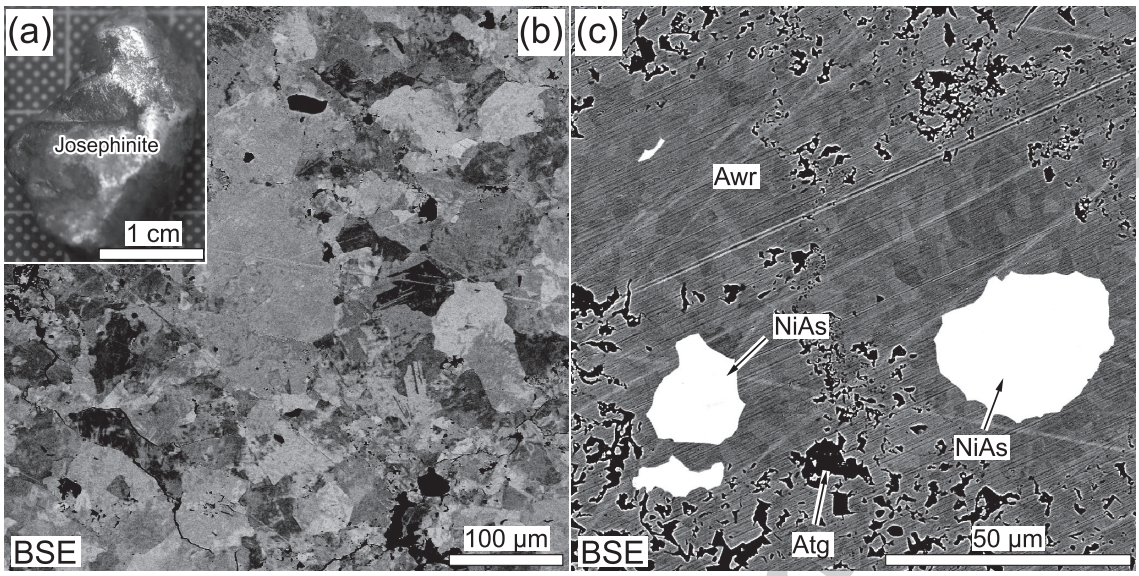

Figure 2. Textural features of the investigated josephinite sample JOS. (a) A photograph of a josephinite nugget from Josephine Ophiolite. (b) A back-scattered electron (BSE) image of aggregates of awaruite in josephinite. (c) A BSE image showing Ni-arsenide enclosed within awaruite.

Table 1. Representative chemical composition of awaruite in sample JOS analyzed by FE-EPMA

Spots	A-1	A-2	A-3	A-4	A-5	A-6	A-7	A-8
wt%								
Si	–	–	–	–	–	–	–	–
Cr	–	–	–	–	–	–	–	–
O	–	–	–	–	–	–	–	–
Cu	0.95	1.09	0.93	1.05	0.71	0.73	0.98	0.70
Fe	23.56	24.32	24.09	24.21	24.58	25.82	24.51	26.12
Al	–	–	–	–	–	–	–	–
Mn	0.01	0.02	0.01	–	–	–	–	–
As	0.10	0.05	0.15	0.02	0.22	0.09	0.12	0.15
Co	0.40	0.43	0.38	0.41	0.44	0.50	0.37	0.53
Ni	74.93	73.74	74.81	74.31	74.61	73.18	74.78	73.18
S	0.01	0.28	–	0.25	–	–	–	0.01
Total	99.97	99.93	100.37	100.26	100.56	100.31	100.76	100.69
atomic%								
Si	–	–	–	–	–	–	–	–
Cr	–	–	–	–	–	–	–	–
O	–	–	–	–	–	–	–	–
Cu	0.87	0.99	0.85	0.96	0.65	0.66	0.89	0.63
Fe	24.50	25.24	24.95	25.05	25.40	26.72	25.29	26.93
Al	–	–	–	–	–	–	–	–
Mn	0.02	0.02	0.01	–	–	–	–	–
As	0.08	0.04	0.12	0.02	0.17	0.07	0.09	0.11
Co	0.40	0.42	0.38	0.41	0.43	0.49	0.36	0.52
Ni	74.13	72.79	73.71	73.12	73.35	72.06	73.37	71.78
S	0.01	0.51	–	0.45	–	–	–	0.021
Total	100.00	100.00	100.00	100.00	100.00	100.00	100.00	100.00

and illustrated in Figure 4. The Pb isotope ratios of leachates (L1 and L5) and the earlier steps of partial dissolution (PD7 to PD11) are variable. This suggest that the Pb isotope ratios of the leachates (L1 and L5) and the earlier steps of the partial dissolution steps (PD7 to PD11) may represent an altered signature. However, all ratios converge to a homogeneous value towards the later steps of the partial dissolution (PD12 to PD 17). This homogeneity allowed to calculate weighted mean values that gives the primordial Pb isotope ratios. Using a R package 'IsoplotR' (Vermeesch, 2018), we obtained $^{206}Pb/^{204}Pb$ = 18.3283 ± 0.0020 (MSWD = 0.49), $^{207}Pb/^{204}Pb$ = 15.5645 ±

Advance Publication

Table 2. Representative chemical composition of Ni-arsenide in sample JOS analyzed by FE-EPMA

Spots	B-33	B-34	B-35	B-36	B-37	B-38
wt%						
Si	–	–	–	–	–	–
Cr	–	–	–	–	–	–
O	–	–	–	–	–	–
Cu	–	–	–	–	–	–
Fe	0.89	0.60	2.70	3.44	4.27	3.33
Al	–	–	–	–	–	–
Mn	0.01	0.02	0.02	0.03	0.02	–
As	31.74	31.69	31.85	31.77	31.92	32.19
Co	0.01	–	0.02	–	0.063	0.029
Ni	67.03	67.02	64.74	64.73	64.06	64.13
S	–	–	–	–	–	–
Total	99.67	99.32	99.32	99.97	100.33	99.68
atomic%						
Si	–	–	–	–	–	–
Cr	–	–	–	–	–	–
O	–	–	–	–	–	–
Cu	–	–	–	–	–	–
Fe	1.01	0.68	3.06	3.88	4.788	3.77
Al	–	–	–	–	–	–
Mn	0.01	0.02	0.02	0.03	0.02	–
As	26.79	26.85	26.96	26.69	26.71	27.16
Co	0.01	–	0.02	–	0.07	0.03
Ni	72.19	72.45	69.94	69.40	68.41	69.04
S	–	–	–	–	–	–
Total	100.00	100.00	100.00	100.00	100.00	100.00

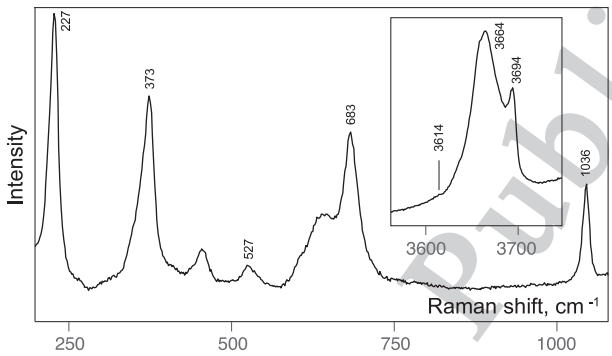

Figure 3. Raman spectrum of antigorite from josephinite-bearing host serpentinite sample SRP.

0.0020 (MSWD = 0.36), and $^{208}Pb/^{204}Pb$ = 38.0723 ± 0.0061 (MSWD = 0.50).

DISCUSSION

A new interpretation on Pb isotope ratios of josephinite

In Figure 5, the Pb isotope ratios of josephinite obtained in this study are shown together with those of Göpel et al. (1990). The newly obtained Pb isotope ratios of josephinite indicates that it is enriched in $^{207}Pb/^{204}Pb$ ratio with MORB source-like $^{206}Pb/^{204}Pb$ and $^{208}Pb/^{204}Pb$ ratios, which show a consistency with the previous study (Göpel et al., 1990). They reported that the Pb isotope ratios of josephinite overlap with those from the diorite intrusions associated with the Josephine Ophiolite and suggested that Pb isotope features of josephinite-forming fluid may reflect arc magmatic processes. Similar Pb isotope ratios were reported from the back-arc seamounts in the central Izu-Bonin intra-oceanic arc (Ishizuka et al., 2003).

However, josephinite contains Ni-arsenide inclusions (Botto and Morrison, 1976; this study). The presence of Ni-arsenide indicates the infiltration of As-bearing fluids during or prior to the awaruite crystallization. Deschamps et al. (2012) studied bulk-rock trace elements geochemistry of serpentinites from Cuba and Dominican Republic. They reported remarkable enrichments of As and Sb only in antigorite-bearing subducted serpentinites. The As enrichment was also reported in an eclogite-bearing, antigorite serpentinites in the Tso Morari region of NW Himalayas (Hattori et al., 2005). Those extreme enrichment of As in antigorite serpentinites was interpreted as an input of As due to the involvement of sediment-derived fluids with high As concentration. In addition, in case of Cuba and Dominican Republic occurrence, the geochemical fingerprint of sediment-derived fluids was also supported by high $^{207}Pb/^{204}Pb$ ratios (Deschamps and Hattori, 2013). Considering the presence of Ni-arsenide and the enriched $^{207}Pb/^{204}Pb$ ratios in josephinite, the involvement of sediment-derived fluids to the josephinite formation cannot be ruled out.

Perspectives

Awaruite is the most common Ni-Fe alloy found in serpentinite and/or serpentinized peridotite. It is well known that hydrogen can be produced during the initial stages of low-temperature serpentinization, which forms serpentine and magnetite from Fe-rich brucite (e.g., Bach et al., 2004; Sleep et al., 2004; Frost and Beard, 2007; Klein et al., 2009). Such Hydrogen-bearing fluids are considered to buffer the reduced environment in serpentinite that can form alloys such as awaruite.

The presence of antigorite in josephinite-hosting serpentinites suggests that local awaruite concentration processes to form josephinite take place in a stability field of antigorite at a temperature of ~ 350-500 °C (e.g., Guillot et al., 2015). However, awaruite has been reported in low-temperature hydrothermally altered ocean floor serpentinites since the early time of serpentinite studies and was also considered to form in orogenic antigorite serpentinites (Hultin, 1968; Trommsdorff and Evans, 1977). Recently, Milidragovic and Grundy (2019) reported the occurrence of awaruite within a large body of antigorite-bearing serpentinite of Trembleur ultramafic unit from

Advance Publication Article

Table 3. Representative chemical composition of antigorite in sample SRP analyzed by FE-EPMA

Spots	A-1	A-2	A-3	A-4	A-9	A-10	A-11	A-12
SiO_2	44.70	44.33	44.75	44.44	41.73	43.81	43.48	43.47
TiO_2	0.02	0.05	0.08	–	0.04	–	–	0.01
Al_2O_3	0.37	0.43	0.41	0.39	0.27	0.19	0.18	0.30
Cr_2O_3	0.08	0.12	0.18	0.09	0.14	0.15	0.02	0.12
FeO	4.53	4.75	4.68	5.42	3.88	3.13	2.87	3.92
MnO	–	0.18	–	–	0.09	0.08	–	–
MgO	37.30	37.38	37.16	37.58	37.13	39.34	39.27	37.60
NiO	0.19	0.20	0.23	0.28	1.25	0.51	0.88	1.17
CaO	0.04	0.03	–	0.01	0.11	0.02	–	0.01
Total	87.24	87.48	87.49	88.22	84.63	87.24	86.70	86.60
Atomic per formula unit (O = 14)								
Si	4.178	4.146	4.176	4.135	4.059	4.090	4.087	4.115
Ti	0.002	0.003	0.005	–	0.003	–	–	0.001
Al	0.041	0.047	0.045	0.043	0.030	0.021	0.020	0.033
Cr	0.005	0.009	0.013	0.007	0.011	0.011	0.002	0.009
Fe^{2+}	0.355	0.371	0.365	0.422	0.315	0.244	0.225	0.310
Mn	–	0.014	–	–	0.007	0.006	–	–
Mg	5.198	5.212	5.168	5.212	5.383	5.475	5.502	5.305
Ni	0.014	0.015	0.017	0.021	0.098	0.038	0.066	0.089
Ca	0.004	0.003	–	0.001	0.011	0.002	–	0.002
Total	9.797	9.821	9.790	9.840	9.917	9.888	9.902	9.863
$Mg/(Mg + Fe^{2+})$	0.94	0.93	0.93	0.93	0.94	0.96	0.96	0.94

Table 4. Pb isotope ratios of leachates and etched solutions of sample JOS

	$^{206}Pb/^{204}Pb$	± 2σ	$^{207}Pb/^{204}Pb$	± 2σ	$^{208}Pb/^{204}Pb$	± 2σ
Leachate						
L1	18.219	± 6	15.601	± 6	38.050	± 15
L5	18.248	± 5	15.563	± 5	38.004	± 15
Etched solution						
PD7	18.305	± 5	15.577	± 5	38.083	± 28
PD8	18.357	± 6	15.580	± 5	38.120	± 15
PD9	18.361	± 5	15.572	± 5	38.099	± 15
PD10	18.343	± 6	15.570	± 6	38.091	± 16
PD11	18.352	± 7	15.581	± 7	38.119	± 18
PD12	18.330	± 5	15.561	± 5	38.061	± 15
PD13	18.330	± 6	15.562	± 5	38.063	± 15
PD14	18.332	± 5	15.568	± 5	38.084	± 15
PD15	18.331	± 5	15.568	± 5	38.084	± 15
PD16	18.324	± 5	15.563	± 5	38.065	± 15
PD17	18.324	± 5	15.565	± 5	38.077	± 15
Weighted mean						
	18.3283	± 20	15.5645	± 20	38.0723	± 61

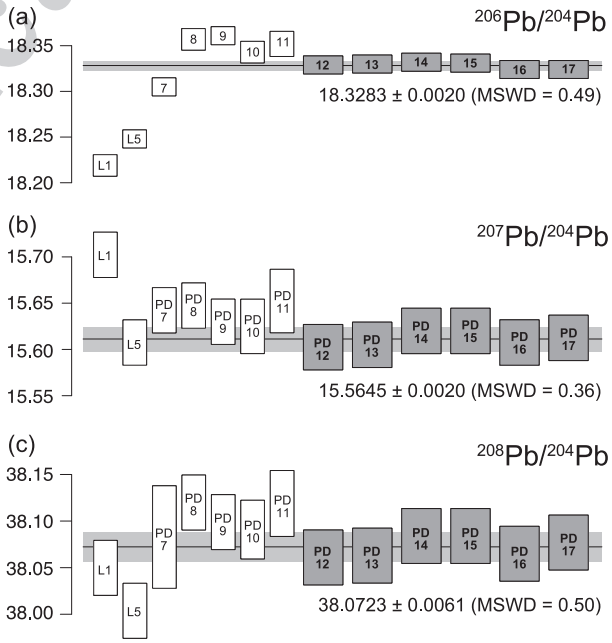

Figure 4. Plots showing the results of Pb isotope ratios of leachates solution (L1 and L5) and etched solutions of partial dissolution steps (PD7 to PD17). The vertical line and the surrounding shaded band represent the weighted mean values calculated using a R package 'IsoplotR' (Vermeesch, 2018). The weighted means were obtained using each isotope ratio of the later partial dissolution (PD12 to PD 17) shown in grey columns; leaching (L1 and L5) and early partial dissolution steps (PD7 to PD11) shown in white columns with narrow width were omitted from the calculation.

the Cache Creek terrane, central British Columbia, Canada. Furthermore, Foustoukos et al. (2015) conducted laboratory experiments which revealed that awaruite can be stable at relatively high f_{O_2} above QFM buffer, which is in contrast with previous thoughts. These suggest that awaruite may form in serpentinites from diverse tectonic

Advance Publication Article

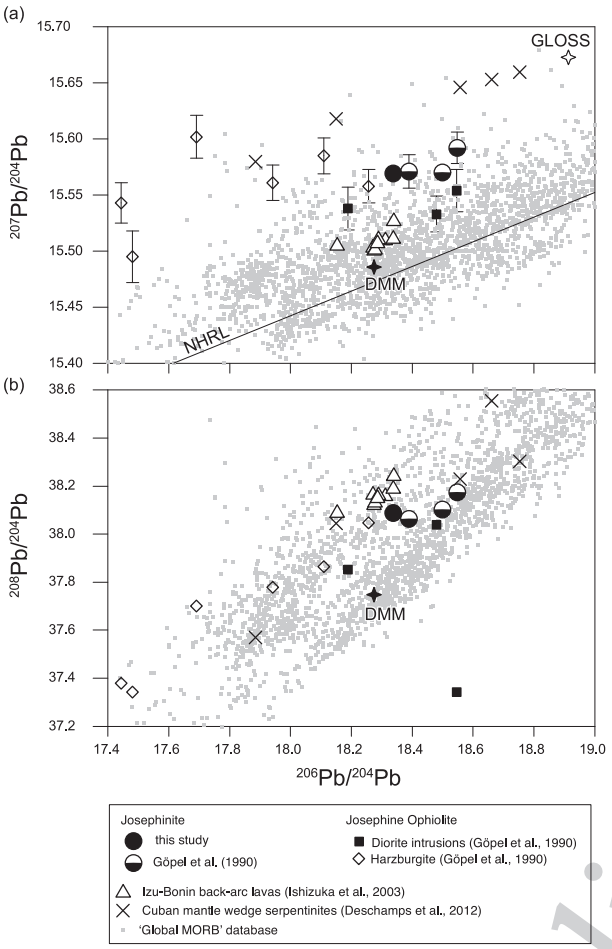

Figure 5. Binary plots of (a) $^{207}Pb/^{204}Pb$ versus $^{206}Pb/^{204}Pb$ and (b) $^{208}Pb/^{204}Pb$ versus $^{206}Pb/^{204}Pb$, showing the Pb isotope ratios of josephinite determined by this study with previously obtained Pb isotope ratios of josephinites (Göpel et al., 1990). In comparison, Pb isotope ratios of the diorite intrusions and the harzburgite in the Josephine Ophiolite (Göpel et al., 1990), Izu-Bonin back-arc volcanics (Ishizuka et al., 2003), Cuban mantle wedge serpentinites (Deschamps et al., 2012), global MORB data from the PetDB Database (http://www.earthchem.org/petdb), GLOSS (Plank and Langmuir, 1998) and DMM (Workman and Hart, 2005) are also shown.

setting under various redox conditions.

Using the weighted mean method, we have newly obtained the precise Pb isotope ratios of josephinite. Our results can be evaluated as one of the references Pb isotope ratios in the SSZ serpentinites. Although, it is believed that Pb isotope ratios of serpentinites can be easily modified by the fluids which are enriched in fluid-mobile elements, a strategy focusing on Pb isotope studies of awaruite would bring a new opportunity to understand fluids evolution in the SSZ serpentinites. To better understand the fingerprints of fluid processes in the SSZ serpentinites, further isotope studies may appear necessary, such as Li, B, Mg, and Fe.

ACKNOWLEDGMENTS

We would like to express special thanks to Robert G. Coleman who provided samples and maps. This research is supported by COLABS program of Tohoku University with oversea travel grants from JASSO to MK. This study is also partially supported by CNEAS of Tohoku University by MEXT/JSPS KAKENHI Grant Numbers JP15H05212 and JP18H01299 to TT, and the MOST 107-2116-M-001-003 to YI. We appreciate for constructive reviews from Gen Shimoda and Tomoaki Morishita. We extend our appreciation to Noriyoshi Tsuchiya and Atsushi Okamoto for their assistance on the micro Raman spectroscopy.

REFERENCES

Amelin, Y. (2008) The U-Pb systematics of angrite Sahara 99555. Geochimica et Cosmochimica Acta, 72, 4874-4885.

Bach, W., Garrido, C.J., Paulick, H., Harvey, J. and Rosner, M. (2004) Seawater-peridotite interactions: First insights from ODP Leg 209, MAR 15°N. Geochemistry, Geophysics, Geosystems, 5, Q09F26, doi:10.1029/2004GC000744.

Bird, J.M. and Weathers, M.S. (1979) Origin of josephinite. Geochemical Journal, 13, 41-55.

Botto, R.I. and Morrison, G.H. (1976) Josephinite; a unique nickel-iron. American Journal of Science, 276, 241-274.

Britten, G.L., Wakamatsu, L. and Primeau, F.W. (2017) The temperature-ballast hypothesis explains carbon export efficiency observations in the Southern Ocean. Geophysical Research Letters, 44, 1831-1838.

Debret, B. and Sverjensky, D.A. (2017) Highly oxidising fluids generated during serpentinite breakdown in subduction zones. Scientific Reports, 7, 10351, doi:10.1038/s41598-017-09626-y.

Deschamps, F., Godard, M., Guillot, S., Chauvel, C., et al. (2012) Behavior of fluid-mobile elements in serpentines from abyssal to subduction environments: Examples from Cuba and Dominican Republic. Chemical Geology, 312-313, 93-117.

Deschamps, F. and Hattori, K. (2013) Geochemistry of subduction zone serpentinites: A review. Lithos, 178, 96-127.

Dick, H.J.B. (1974) Terrestrial nickel-iron from the Josephine Peridotite, its geologic occurrence, associations, and origin. Earth and Planetary Science Letters, 24, 291-298.

Dilek, Y. and Furnes, H. (2011) Ophiolite genesis and global tectonics: Geochemical and tectonic fingerprinting of ancient oceanic lithosphere. Bulletin of the Geological Society of America, 123, 387-441.

Evans, B.W., Hattori, K. and Baronnet, A. (2013) Serpentinite: What, why, where?. Elements, 9, 99-106.

Foustoukos, D.I., Bizimis, M., Frisby, C. and Shirey, S.B. (2015) Redox controls on Ni-Fe-PGE mineralization and Re/Os fractionation during serpentinization of abyssal peridotite. Geochimica et Cosmochimica Acta, 150, 11-25.

Frost, R.B. and Beard, J.S. (2007) On silica activity and serpentinization. Journal of Petrology, 48, 1351-1568.

Göpel, C., Manhès, G. and Allègre, C.J. (1990) U-Pb isotope systematics in josephinites and associated rocks. Earth and Planetary Science Letters, 97, 18-28.

Guillot, S. and Hattori, K. (2013) Serpentinites: Essential roles in

Advance Publication Article

geodynamics, arc volcanism, sustainable development, and the origin of life. Elements, 9, 95-98.

Guillot, S., Schwartz, S., Reynard, B., Agard, P. and Prigent, C. (2015) Tectonic significance of serpentinites. Tectonophysics, 646, 1-19.

Harper, G.D. (1984) The Josephine ophiolite, northwestern California. Geological Society of America Bulletin, 95, 1009-1026.

Hattori, K., Takahashi, Y., Guillot, S. and Johanson, B. (2005) Occurrence of arsenic (V) in forearc mantle serpentinites based on X-ray absorption spectroscopy study. Geochimica et Cosmochimica Acta, 69, 5585-5596.

Hultin, I. (1968) Awaruite (josephinite), a new nineral for Norway. Norsk geologisk tidsskrift, 48, 179-185.

Ishizuka, O., Taylor, R.N., Milton, J.A. and Nesbitt, R.W. (2003) Fluid-mantle interaction in an intra-oceanic arc: Constraints from high-precision Pb isotopes. Earth and Planetary Science Letters, 211, 221-236.

Kamenetsky, V.S., Lygin, A.V., Foster, J.G., Meffre, S., et al. (2016) A story of olivine from the McIvor Hill complex (Tasmania, Australia): Clues to the origin of the Avebury metasomatic Ni sulfide deposit. American Mineralogist, 101, 1321-1331.

Kelemen, P.B. and Dick, H.J.B. (1995) Focused melt flow and localized deformation in the upper mantle: juxtaposition of replacive dunite and ductile shear zones in the Josephine peridotite, SW Oregon. Journal of Geophysical Research, B1, 100, 423-438.

Klein, F., Bach, W., Jöns, N., McCollom, T., et al. (2009) Iron partitioning and hydrogen generation during serpentinization of abyssal peridotites from 15°N on the Mid-Atlantic Ridge. Geochimica et Cosmochimica Acta, 73, 6868-6893.

Kodolányi, J., Pettke, T., Spandler, C., Kamber, B.S. and Ling, K.G. (2012) Geochemistry of ocean floor and fore-arc serpentinites: Constraints on the ultramafic input to subduction zones. Journal of Petrology, 53, 235-270.

Lugmair, G.W. and Galer, S.J.G. (1992) Age and isotopic relationships among the angrites Lewis Cliff 86010 and Angra dos Reis. Geochimica et Cosmochimica Acta, 56, 1673-1694.

Martin, L.A.J., Wood, B.J., Turner, S. and Rushmer, T. (2011) Experimental measurements of trace element partitioning between lawsonite, zoisite and fluid and their implication for the composition of arc magmas. Journal of Petrology, 52, 1049-1075.

Milidragovic, D. and Grundy, R. (2019) Geochemistry and petrology of rocks in the Decar area, central British Columbia: Petrologically constrained subdivision of the Cache Creek complex. Geological Fieldwork 2018, British Columbia Ministry Of Energy, Mines, and Petroleum Resources, British Columbia Geological Survey Paper, 55-77.

Oyanagi, R., Okamoto, A., Hirano, N. and Tsuchiya, N. (2015) Competitive hydration and dehydration at olivine-quartz boundary revealed by hydrothermal experiments: Implications for silica metasomatism at the crust-mantle boundary. Earth and Planetary Science Letters, 425, 44-54.

Peters, D., Bretscher, A., John, T., Scambelluri, M. and Pettke, T. (2017) Fluid-mobile elements in serpentinites: Constraints on serpentinisation environments and element cycling in subduction zones. Chemical Geology, 466, 654-666.

Plank, T. and Langmuir, C.H. (1998) The chemical composition of subducting sediment and its consequences for the crust and mantle. Chemical Geology, 145, 325-394.

Plümper, O., Botan, A., Los, C., Liu, Y., et al. (2017) Fluid-driven metamorphism of the continental crust governed by nanoscale fluid flow. Nature Geoscience, 10, 685-690.

Ramp, L. (1986) Geologic map of the northwest quarter of the Cave Junction quadrangle, Josephine County, Oregon. Oregon Department of Geological and Mineral Industries Geological Map Series GMS-38, scale 1:24,000.

Reynard, B. (2013) Serpentine in active subduction zones. Lithos, 178, 171-185.

Le Roux, V., Dick, H.J.B. and Shimizu, N. (2014) Tracking flux melting and melt percolation in supra-subduction peridotites (Josephine ophiolite, USA). Contributions to Mineralogy and Petrology, 168, 1-22.

Scambelluri, M., Müntener, O., Ottolini, L., Pettke, T.T. and Vannucci, R. (2004) The fate of B, Cl and Li in the subducted oceanic mantle and in the antigorite breakdown fluids. Earth and Planetary Science Letters, 222, 217-234.

Sleep, N.H., Meibom, A., Fridriksson, T., Coleman, R.G. and Bird, D.K. (2004) H2-rich fluids from serpentinization: Geochemical and biotic implications. Proceedings of the National Academy of Sciences, 101, 12818-12823.

Trommsdorff, V. and Evans, B.W. (1977) Antigorite-ophicarbonates: Contact metamorphism in Valmalenco, Italy. Contributions to Mineralogy and Petrology, 62, 301-312.

Vermeesch, P. (2018) IsoplotR: A free and open toolbox for geochronology. Geoscience Frontiers, 9, 1479-1493.

Workman, R.K. and Hart, S.R. (2005) Major and trace element composition of the depleted MORB mantle (DMM). Earth and Planetary Science Letters, 231, 53-72.

Yamada, C., Tsujimori, T., Chang, Q. and Kimura, J.I. (2019a) Boron isotope variations of Franciscan serpentinites, northern California. Lithos, 334-335, 180-189.

Yamada, C., Tsujimori, T., Chang, Q. and Kimura, J.-I. (2019b) Boron isotope compositions of antigorite-grade serpentinites in the Itoigawa-Omi area of the Hida-Gaien Belt, Japan. Journal of Mineralogical and Petrological Sciences, 114, 290-295.

Manuscript received July 31, 2019
Manuscript accepted January 26, 2020

Manuscript handled by M. Satish-Kumar

Advance Publication Article